Journal of Sustainable Development of Energy, Water and Environment Systems

http://www.sdewes.org/jsdewes

Year 2024, Volume 12, Issue 4, 1120520

Original Research Article

Optimisation of Wastewater Treatment Plant Based on Polymer and Electricity Consumption − a Case Study of Finland

***Ana Carolina Méndez-Ecoscia*[*1], *Javier Farfan*[2], *Carl-Eric Wilén*[1], *Henrik Sáxen*[2]**

[1]Faculty of Science and Engineering, Laboratory of Molecular Science and Engineering, Åbo Akademi University, Henrikinkatu 2, 20500 Turku, Finland

e-mail: ana.mendezecoscia@abo.fi

[2] Faculty of Science and Engineering, Laboratory of Process and Systems Engineering, Åbo Akademi University, Henrikinkatu 2, 20500 Turku, Finland

e-mail: francisco.farfanorozco@abo.fi

Cite as: Méndez-Ecoscia, A. C., Farfan Orozco, F. J., Wilén, C. E., Saxén, H., Optimization of wastewater treatment plant based on polymer and electricity consumption - A case study of Finland, J.sustain. dev. energy water environ. syst., 12(4), 1120520, 2024, DOI: https://doi.org/10.13044/j.sdewes.d12.0520

ABSTRACT

Wastewater treatment plants are crucial for water management, enabling water reuse, recycling, and regulating pollutant levels. Their operation varies based on factors such as season, wastewater type, and treatment volume, impacting electricity and material consumption. Despite their longstanding use, chemical agents are often applied at constant ratios, resulting in excessive use and environmental impact. A model was employed to analyse plant operation, focusing on optimising polymer concentration and electricity demand. Polymer reduction was monitored through sedimentation kinetics at different concentrations, incorporating zeta potential measurement and particle size distribution. Sedimentation data were interpreted using a TurbiScan Lab®, examining the effect of sample collection and analysis time on sedimentation kinetics. The optimal cationic polyacrylamide concentration for treating wastewater with approximately 5 mg/L suspended particles and 5.525 mg/mL phosphorus ranged from 0.1 mg/mL to 1.3 mg/mL. In-line sensing of suspended particles can optimise polymer use. Additionally, a novel electricity operation mode was tested in a Finnish plant, presenting a model that can be extrapolated to enhance global wastewater treatment operations.

KEYWORDS

Wastewater treatment, Process optimisation, Kinetics, Stability, Polymer, Electricity, Cost reduction, Environment.

INTRODUCTION

With the growing environmental awareness of society, the implementation of environmentally friendly alternatives and thoughtful strategies is no longer a choice, but a necessity. Evaluating everyday activities has become a must. This is particularly relevant when discussing water resources management [1]. Wastewater treatment plants play an essential role in municipalities as they facilitate water reuse and recycling. Overall, they help maintain a safe level of pollutants released into the environment. However, like every industrial plant, they require energy and chemical compounds to operate and inevitably release emission into the atmosphere [2].

Even though the treatment technology principle of the Wastewater Treatment Plant (WWTP) has been known for more than 50 years, recent advances in instrumentation, chemical

* Corresponding author

analysis, and online monitoring are paving new path for research and process optimisation [3]. However, these improvements are far from straightforward; the complex and variable nature of the incoming water makes wastewater treatment plants challenging subjects of study [4]. Influent characteristics may change depending on the season, human activities, and population growth. Moreover, understanding of the water-energy nexus in the traditionally compartmentalised wastewater treatment industry is key to developing an efficient, cost-effective and sustainable process [5].

Technological advancements are leading to the implementation of on-line monitoring and control systems in the wastewater treatment industry. Nowadays, integrated systems allow for overcoming traditional static water management by not only providing real-time monitoring and control but also by storing data that can be further utilised for network-wide distribution and create new variables correlations [6]. Certainly, the connection of devices into the network needs to be backed up by a system that can be manually operated and complemented with offline samplings to guarantee performance and avoid disruptions in the operation of the wastewater treatment plant, all while maintaining the compliance with pollutant levels contained in the water prior to releasing it into the environment [4]. Therefore, the availability of this data smoothens plant operation by facilitating the decision-making thanks to the integration of the traditional water quality standards (total solids, total nutrients, pH, oil products, particle size, metal concentration) with key process parameters (mass balance, mixing, residence time, energy demands) [6], and addresses new monitoring needs such as multidirectional communication between sensors and continuous retrofit [7]. Additionally, more sophisticated analytical methods and new concerns are paving the way for integrating new water quality variables based on the control of emerging pollutants such as phthalates, Bisphenol A, and pharmaceuticals [8].

While chemical treatments are beginning to be replaced by membrane technology, the chemical segment of the global wastewater treatment industry accounted for $46.2 billion in 2022 [9]. Chemical treatment processes are divided into chemical precipitation, neutralisation, adsorption, disinfection and ion exchange [10]. In this context, pH neutralisers, anti-foaming agents, coagulant and flocculants are the main types of chemicals used in the wastewater treatment process [11]. pH neutralisation is added to the process to prevent undesirable chemical reactions that can occur due to the mixing between the wastewater effluent and other sub-process streams [11]. Neutralisation is particularly important to meet the regulatory specification of water discharge into lakes or rivers [12]. Anti-foaming agents, on the other hand, can be seen as process adjuvant since their presence maintains operational efficiency and reduces process costs by limiting deposits inside storage tanks and processing vessels. In this way, bacterial growth is limited while ensuring worker safety [13]. This study shifts its focus to the examination of chemicals that intervene in the coagulation/flocculation process and affect the separation process between the suspended particles and water.

Coagulation, the first step of the process, involves colloidal destabilisation, followed by the initiation of flocculation when destabilised particles begin to propagate and agglomerate. The mechanisms of destabilisation are related to the nature of the coagulant employed [14]. This article does not cover the optimisation of coagulant amount. Instead, it focuses on the screening of cationic polymers used in the flocculation process. The wastewater treatment plant chosen for evaluated the proposed methodologies, adds ferrous sulphate for secondary clarification at a rate of 30 g/m^3. All the samples studied contained this concentration of coagulant before conducting the flocculation studies. It is well known that in presence of cationic polymer, particle destabilisation is achieved by the charge neutralisation mechanism, but interparticle bridging also plays a significant role. In simple terms, flocculation by polymer bridging occurs when the active polymer attaches to a free surface particle. When the particles attach, the distance between them reduces, thereby increasing the frequency of collision. Therefore, in the presence of higher concentration of “active” particles the probabilities of creating these bonds increases [15].

Polyacrylamides (PAM) are commonly employed in water treatment processes. Despite their widespread use, there is not an established standard method to determine their traces in water [16]. Detection of polyacrylamides in solution requires complex sample preparation to ensure detection levels, and in some cases, reproducibility cannot be ensured. So far, the incorporation of a fluorescence marker appears to be the most suitable technique to ensure accuracy and reproducibility by adding a fluorescence tag, the ions coming from the functional groups of the polymer will be selectively enhanced, and detection can be achieved. For example, in patent US6514617B1 [17] a tagging material obtained from the combination of one fluorophore dye and one semi-conducting luminesce nanoparticle allows the identification of polymer via spectrofluorometer. A similar approach to detect and control the dosage of polymers was proposed in the patent US20010018503A1 [18], where the fluorescence tag is derived from a water-in-oil emulsion tag that is later incorporated into the polymer. Swift et al. [19] proposed the use of interpolymer complexation to monitor the polymer concentration of PAM. The advantage of this method is that interpolymer complexation can be easily achieved by mixing polymers. The inter-polymerisation occurs thanks to the structure similarity between the PAM and the polymer complex; in this case, poly (acrylic acid-co-acenaphthylene). It is also possible that the required amounts of the fluorescence tag to be added are low, which directly implies an economically viable alternative. According to the guidelines for drinking-water quality [20], the maximum polyacrylamide concentration in water is 1 mg/L, while the monomer concentration should not exceed 0.5 µg/L (i.e., 0.05% of the monomer content of residual monomer in polymer). To summarize, avoiding excessive amounts of polymer constitutes the most efficient alternative to limit the potential detrimental effect that the degradation of this polymer can have on the environment. The optimisation of the concentration of polyacrylamides was one of the drivers of the current study.

Recognising the critical relationship between water and energy is key to achieving sustainable resource management [5]. Wastewater treatment is a highly energy-consuming process [21] to propose cost reduction by more efficiently controlling electricity demands. The optimisation of these demands needs to ensure continuous operation by guaranteeing process performance [22]. In this context, the use of Energy Storage Systems (EES) has been recognised as an viable option to provide an optimal balance between energy supply and demand, while improving net carbon emissions [23]. In practice, the role of the EES is to store energy and use it whenever and wherever needed [23]. For instance, when the energy supply exceeds demand, it can be beneficial to store the energy and then utilize that energy when the scenario is reversed [23]. This approach can help eradicate problems associated with peak load and other power supply disturbances [23]. Clearly, storage systems allow for integration and flexible handling of market demands. The suitability of a specific storage system involves evaluating several factors, such as application type, application period, maintainability demands, reduction of the performance after charge-discharge cycles, efficiency and capital cost [24]. Another important factor when implementing a sustainable approach is to include the circularity approach. Therefore, the decommissioning and removal of chemicals contained in the batteries is playing a crucial role in technology selection [25] the need for new recycling approaches is currently experiencing significant development [26].

Given the importance of integrating chemical and energy approaches to optimize the operation of the wastewater treatment plant, this study identifies a significant gap in the current practices. The primary objective is to explore alternatives that enable the implementation of a more cost-efficient water treatment process. This exploration is grounded in a real-world case study: a wastewater treatment plant located in Turku, Finland. The detrimental effects of excessive polymer presence in the ecosystem and the high energy consumption of a water treatment plant are key considerations.

The first part of this study is dedicated to reducing the amount of polymer used in the secondary clarification step. This is achieved by enhancing the understanding of the impact of the flocculant and residence time on the kinetic profiles of the secondary clarification unit. The

second part of this study evaluates the potential for cost reduction and operational flexibility that can be achieved by implementing an energy storage system. Specifically, the installation of a grid-scale battery is proposed. This guarantees the continuous operation of the plant by capitalising on fluctuating electricity prices in the market.

In essence, this study introduces two novel approaches aimed at optimising the operation of wastewater treatment plants. The first approach focuses on determining the optimal amount of polymer required for plant operation. This is achieved by monitoring parameters such as zeta potential, particle size evolution, turbidity, and metal ion concentration using Inductively Coupled Plasma Optical Emission Spectroscopy (ICP-OES). The goal is to ensure the expected safety and quality attributes of the treated water. The second approach proposes the use of a grid-scale battery to reduce electricity costs associated with plant operation. This method not only guarantees the continuous operation of the plant but also significantly reduces energy costs. These methodologies, when implemented, could lead to more efficient and cost-effective wastewater treatment processes. The following sections provide a detailed discussion of these approaches and their potential impact on wastewater treatment.

METHODS

Optimisation of the chemical agent: polymer

In this study, two strategies were pursued to gain an understanding of the kinetic of flocculation triggered by the cationic polymer. The first strategy was based on the measurement of the zeta potential, and the second was based on the particle migration via turbidity measurement. Additionally, to understand the growth of flocs after polymer addition, particle size distribution measurement was also performed.

Materials. The general characteristics of the water samples used for this study are summarised in **Table 1**. Water samples were provided by Turku WWTP (Turun Seudun Puhdistamo). Grab samples were collected from one of the mixing tanks located just after the aeration unit and before the secondary clarification step (**Figure 6**).

Table 1. Reference values of the selected wastewater samples collected in the mixing take after the aeration step between 9 AM and 10 AM

Series name	Suspended solids [mg/L]	Inflow [m^3/h]	Ammonium [mg/L]	Nitrate [mg/L]
09-01-2023	4.72	877	0.1	5.6
23-01-2023	5.22	1223	0.5	2.9
25-01-2023	4.96	1191	0.5	2.8
30-01-2023	5.01	1339	0.8	2.9
20-02-2023	4.77	838	0.5	3.8

The optimisation of the analytical approach, the delay between sample collection and analysis, as well as the reproducibility study, were successfully validated for the data shown in this article. Therefore, samples collected on January 25th, January 31st, and February 20th were used to draw the conclusions presented in this preliminary flocculant assessment. Additionally, commercial cationic polymers FLOPAM FO 4490 SH, FLOPAM FO 4700 SH, FLOPAM FO 4990 SH and FLOPAM FO 4650 SSH used for the screening study were provided by SNF Finland.

Zeta potential. Zeta potential was measured using *Zetasizer Nano ZS* from Malvern Instruments, equipped with a folded capillary cell DTS1070. For the titration experiments, an MPT-2 multipurpose titrator and a vacuum degasser equipment were employed. The measurement of the standard calibration solution was carried out before each data set.

Turbiscan. *Turbiscan Lab® Expert* was used to measure the particle migration of the flocs formed after polymer addition. Typically, 10 mL of the solution was placed inside a glass cell. The blank (or reference) sample consisted of 5 mL of raw water and 5 mL of deionised water, thus considering the dilution factor.

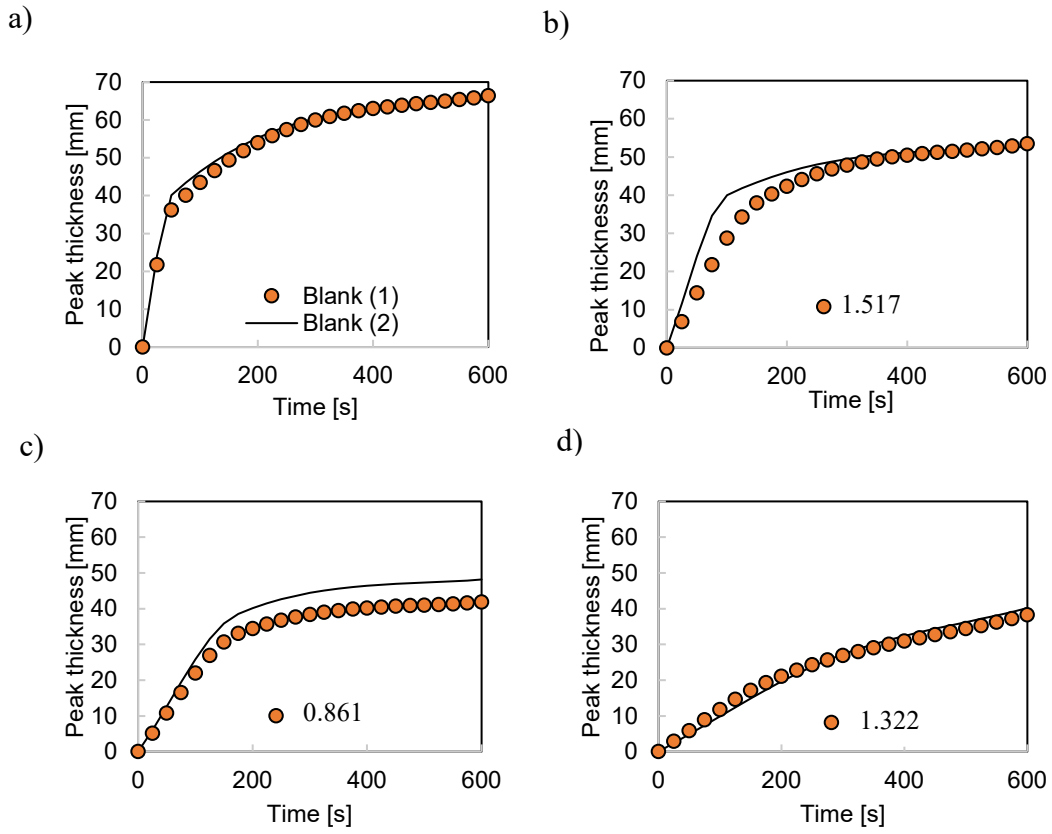

Figure 1. Reproducibility results: evolution of the peak thickness as a function of time, obtained at different polymer concentration: blank, i.e., without polymer (a), 1.517 mg/mL of polymer (b), 0.861 mg/mL of polymer (c), and 1.322 mg/mL of polymer (d)

On an industrial scale, the secondary treatment unit has a very low agitation speed. Therefore, shear-induced flocculation can be neglected, and in the analysis presented here, the focus is on Brownian-induced flocculation. To mimic this phenomenon on a laboratory scale, a fast hand mixing of the raw water and the solution with the specific concentration of polymer was performed just before scanning the sample via the Turbiscan. After data treatment of the backscattering and transmission, the particle migration was computed. Reproducibility was performed to validate the method. For illustration purpose, **Figure 1** shows a part of the results obtained at different polymer concentrations: 0 mg/mL, 1.517 mg/mL, 0.861 mg/mL, and 1.322 mg/mL.

In this study, commercially available polyacrylamide copolymers were used as flocculants. One criterion for choosing the most suitable cationic polymer was based on the zeta potential value. **Figure 2** shows the evolution of the zeta potential as a function of the pH value for three different polymers of medium molar mass "series SH" between 6×10^6 and 8×10^6 g/mol and one with high molar mass "SSH type" between 8×10^6 to 10×10^6 g/mol. As demonstrated below, all polymers have different cationic charges:

- FLOPAM FO 4490 SH − cationic charge = 40%,
- FLOPAM FO 4700 SH − cationic charge = 70%,
- FLOPAM FO 4990 SH − cationic charge = 100%,
- FLOPAM FO 4650 SSH − cationic charge = 55%.

As expected, the isoelectric point (where zeta potential = 0 mV) is dependent on the cationic charge of polymer. Lower pH values are needed to neutralise the charges coming from the impurities for the polymer with the lower cationic charge, as the barrier properties provided by the surrounding layer are thinner. In the case of the polymer form the series SSH, the series with highest molecular weight, the effect of the charge carrier of the monomer unit on the isoelectric point can be observed. For this study, FLOPAM 4650 SSH was employed for the following reasons: 1) the initial zeta potential value of the wastewater samples that were analysed were typically located between −10 mV and −20 mV, 2) the pH of the process was maintained between 6 and 7, and 3) a longer polymer chain enhances flocculation by facilitating bridging with the aggregates.

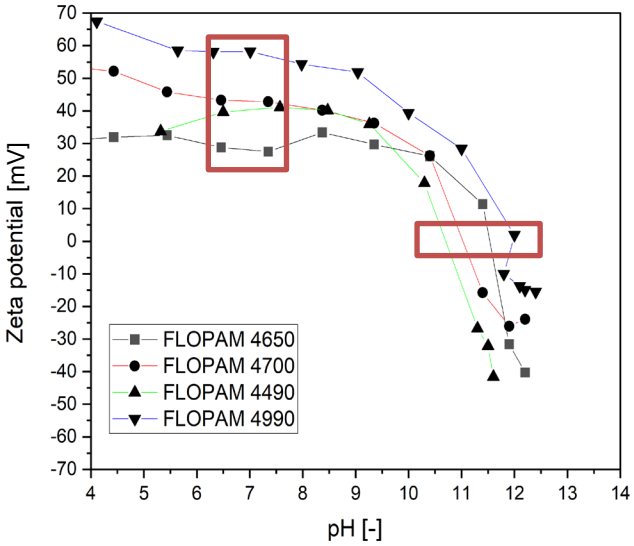

Figure 2. Characterisation of commercially available cationic polymers: evolution of the zetapotential as a function of pH

Particle size distribution..The particle size distribution (PSD) was determined through laser diffraction using a Mastersizer 3000® from Malvern Instruments. The reported PSDs represent the mean of five measurements per sample.

Inductively Coupled Plasma Optical Emission Spectroscopy. Inductively Coupled Plasma Optical Emission Spectroscopy (ICP-OES) using an Optima 5300 DV from Perkin Elmer served to quantify the concentrations of phosphorus, sodium and sulphur. Standards were prepared at concentrations of 1, 5 and 20 ppm. Prior to analysis, all the samples underwent microwave digestion for approximately one hour with 8 mL of 65% HNO_3 (Suprapur®) and 2 mL of 30% H_2O_2.

Optimisation of the electricity costs through grid-scale battery

The Wastewater Treatment Plant (WWTP) in Turku, Finland, showcases a broad spectrum of innovations. The energy-related innovations implemented by the WWTP include:

- Recovery of heat from the treated wastewater,
- Installation of solar panels on the control building,
- Use of geothermal heat pump to generate a significant portion of district heating,
- Location of the entire treatment facility several meters below surface, thereby maintaining operational temperature without the need for heating or cooling,
- Processing of produced sludge to recover energy (in the form of synthetic fuels) and nutrients.

As a result of these practices, the power plant operates in an energy-positive manner, meaning it returns more energy to the system than it consumes [27]. However, the energy returned to the system by the WWTP is in the form of synthetic fuels and district heating, while the energy consumed by the system is electricity. Therefore, despite the system being energy-positive, electricity costs still account for 14% of the plant's operational costs [27]. Historically, the plant has operated using the hourly market electricity price [29], which is the lowest cost option for electricity purchasing in the long term compared to fixed-cost agreements. These hourly electricity market cost fluctuations, illustrated in **Figure 3**, are influenced by factors such as the weather, expected demand, and availability of operating power plants (some of which may be under maintenance). In 2022 in Finland, the maximum hourly price of electricity was 106.78 Euro cents per kWh, while the minimum was negative 0.21 Euro cents per kWh.

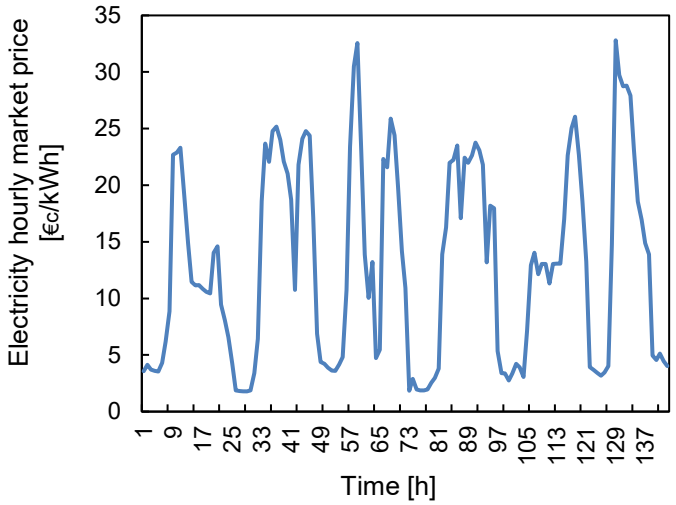

Figure 3. Example of electricity price fluctuations, in Euro cents per kWh, in Finland over a week in September 2022

The proposed cost optimisation strategy for electricity involves the following. Given the constant operational nature of the plant and the daily fluctuations in electricity prices in Finland, connecting the WWTP to a grid-scale battery could significantly reduce the operational electricity cost. By powering the plant directly from the grid and charging the battery during the periods of low electricity prices, and then using the battery to power the plant when electricity prices are high, the operation of the battery can ensure the lowest daily electricity price, thereby significantly reducing the electricity costs.

Considering that the market electricity price is known a day in advance, it is feasible to determine which hours of the day the WWTP would operate from the grid and which hours from the battery. The Turku WWTP uses 11.7 MW for the operation of the entire facility, including the office building and the district heating geothermal heat pump. Taking this into account, and considering that for optimal battery system health the depth of discharge is better maintained at 0.70 [30] for longer battery lifetimes, the battery power capacity was estimated using eq. (1):

$$B_p = \frac{Eh_c}{C_\delta \times B_d} \tag{1}$$

Where B_p denotes the power of the battery in MW, Eh_c signifies the electricity hourly consumption (the 11.7 MW aforementioned), C_δ represents the full cycle efficiency (assumed

as 0.90 in this work) and B_d stands for the end-of-life battery degradation (assumed as 0.80) [31]. Under given data and assumptions, the minimum battery power is 16.25 MW. A battery power is thus chosen as 18 MW for further calculations. It is also assumed that the power for charge and discharge is the same.

The battery storage capacity (BS, in MWh) is subsequently estimated using eq. (2):

$$BS = \frac{B_p \times D_u}{1 - DoD} \tag{2}$$

Where D_u denotes for the daily usage in hours (set as 8 hours for this case study) and DoD signifies for depth of discharge (assumed at 0.70). The resulting minimum required battery storage capacity is thus 480 MWh and is chosen for the case study. Once the battery's power and storage capacities are obtained, the financial assumptions for the grid-scale battery are obtained from [32] and [33].

For the battery operation two scenarios are considered. Scenario 1 considers that the WWTP facility pays the electricity price according to the hourly market as it has been historically done, and Scenario 2 considers a fixed electricity price agreement. For Scenario 1, the battery operation functions charging daily during the 8 hours of lowest cost and discharging (powering the facility) during the 8 hours of highest electricity cost of every day. **Figure 4** shows how the battery would operate under Scenario 1, taking as an example 24 hours of market price of electricity for 16 of September 2022.

In **Figure 4**, the blue line shows the electricity market price of the day (left axis). The yellow line represents the electricity consumption from the grid and the red line is the electricity consumption from the battery system. It can be noted that when the electricity is being taken from the battery, it returns less than what has been taken from the grid. This is due to the return cycle efficiency. In **Figure 4**, in hours 1 to 7 and hour 16 are the lowest prices of electricity that day, thus during those hours both the battery charging, and the powering of the process are directly drawing from the grid. In contrast, hours 8 to 12 and 18 to 22 are the highest market electricity price hours, thus the process is powered by the battery and no electricity is drawn from the grid. Hours 13 to 15 and 22 to 24 the electricity consumption comes exclusively from the grid to the process, as no battery charging takes place at that point.

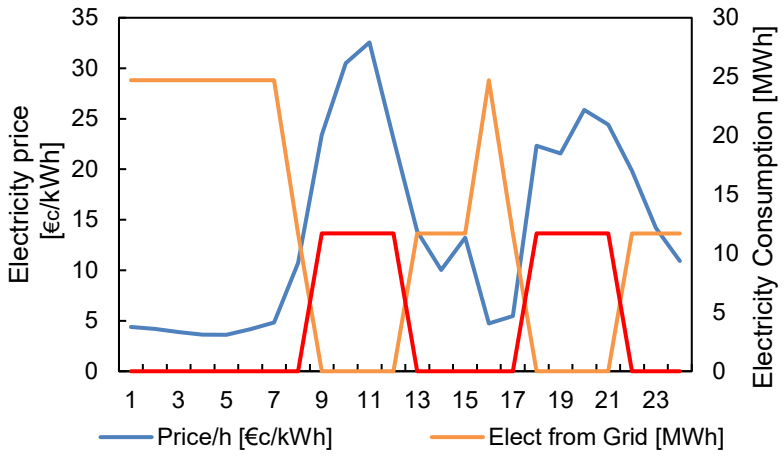

Figure 4. Example of the benefits of battery operation according to scenario 1; the blue line shows the electricity price, the yellow line shows the electricity consumption when charging the battery at the 8 hours lower prices, and the red line shows the electricity discharge during the 8 hours of highest electricity price

For Scenario 1, the lifetime operational cost savings are calculated using eqs. (3) to (5):

$$CR_{S1} = \sum_{1}^{20}\sum_{1}^{365}((DEA_P \times (Eh_c \times 1000) \times 24\ h) - (LC_h + HC_h) \times \frac{1}{C_\delta}))/100 \quad (3)$$

$$LC_h = \left(LFH_{Avg} \times FH_L \times (Eh_c \times 1000)\right) + \left(BD_f \times Nth_{LPH} \times (Eh_c \times 1000)\right) \quad (4)$$

$$HC_h = \left(LGH_{Avg} \times FH_H \times (Eh_c \times 1000)\right) + \left((1 - BD_f) \times Nth_{hPH} \times (Eh_c \times 1000)\right) \quad (5)$$

In eq. (3), CR_{S1} refers to the cost reductions in € of Scenario 1, DEA_p stands for daily mean electricity market price in €/kWh, Eh_c stands for electricity hourly consumption in kWh, LC_h stands for the added daily electricity cost of the lower-cost hours (10 to 8 hours accounting for battery degradation), and HC_h stands for the added daily lower-cost 14 to 16 hours (also accounting for battery degradation).

Eq. (4) describes the electricity cost allocated to the lowest cost hours of the day. LFH_{Avg} stands for the average price of electricity for full load battery hours (for example, at the end of the battery's lifetime is the average price of the lower-cost 8 hours of the day); FH_L stands for full load battery hours (8 at the end of the battery's lifetime); BD_f stands for the battery degradation factor of 0.20 over the 20 years lifetime of the battery, assumed linear, with value from 0 to 1 to account for the partial hours of battery (expected battery capacity of 9.5 hours after the first 5 years of use, for example); Nth_{LPH} stands for the N_{th} lower-cost hour where N is FH_L +1 (for example, after 5 years of operation the battery would charge/discharge 9.5 hours, so FH_L would be 9 and Nth_{LPH} would be the 10th lower-cost hour of the day).

Similar to eq. (4), eq. (5) delineates the cost hours for the duration when the process is powered from the grid. LGH_{Avg} denotes the average price of electricity directly sourced from the grid during the lower-cost full hours of the day, represented by FH_H. For instance, after five years, the battery is projected to provide power for 9.5 hours, leaving 14.5 hours of the day to be powered from the grid, thus FH_H would be 14. Finally, Nth_{hPH} represents the N_{th} lower-cost hour where N equals $FH_H + 1$ (in the example, it would be the 15th lower-cost hour).

In contrast, Scenario 2 contemplates a fixed electricity price agreement. Under this scenario, the battery charges when the market price of electricity falls below the agreed price, and discharges when prices exceed the agreed price (adjusted for cycle efficiency). However, instead of powering the facility, the stored electricity may be sold back to the grid at the market price. **Figure 5** depicts the same day as illustrated in **Figure 4**, but it shows electricity sold back to the grid at revenue margins (represented by the grey line) after adjusting for the electricity purchase at 10 €c per kWh and cycle efficiency. Like Scenario 1, the electricity sale corresponds to the battery degradation-adjusted number of hours with the largest price difference in the day compared to the fixed price. A fixed price of 10 €c per kWh is used as reference, as the specific price agreed cannot be disclosed. Consequently, the revenue under this scenario results from selling electricity from the battery at the margins indicated by the grey line, as calculated using eqs. (6) and (7).

$$CR_{S2} = \sum_{1}^{20}\sum_{1}^{365}\left(\left((EMBh_p \times EB_h) - (E_f \times C_\delta \times EB_h)\right) \times (Eh_c \times 1000)\right)/100 \quad (6)$$

$$EB_h = FB_h \times BD_f \quad (7)$$

Where CR_{S2} stands for collected revenue in Scenario 2, $EMBh_p$ represents the average electricity market price for the battery hours that surpass the furthest the fixed price every day

and E_f stands for the electricity fixed price (at 10 €c for this example), EB_h stands for effective battery hours calculated in eq. (7) as full battery hours (FB_h) multiplied by the battery degradation factor (from 1.00 to 0.80). In **Figure 5** the example can be taken for the hours of that day that selling electricity from the battery to the grid make the most sense.

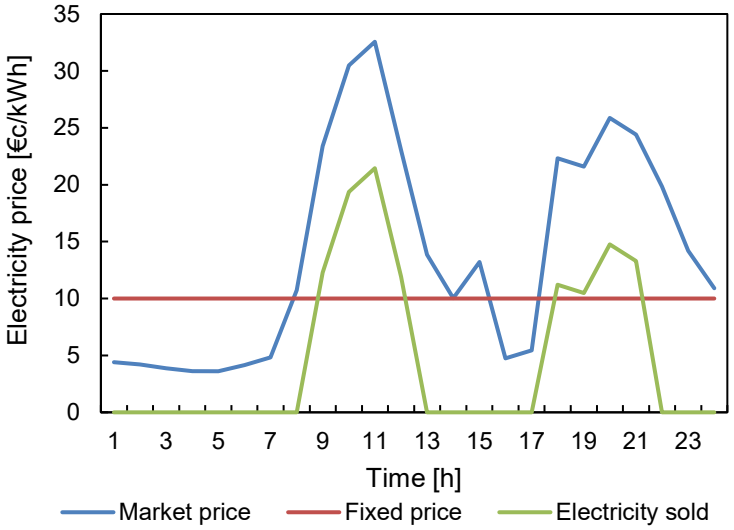

Figure 5. Battery operation to benefit from sales of electricity to the grid when the electricity price rises significantly above the contracted fixed price

Case study data

The plant under study is situated in Turku, Finland, servicing an area of 3,556,930 m^2, covering 300,000 inhabitants and the industry of the region, spanning a total of 14 municipalities [27]. The total input reference flow of the plant can vary from 96,238 m^3/day to 63,263 m^3/day through the year. This input flow is then divided into 4 streams, implying that the reference flow per stream is about 28,500 m^3/day [27]. **Figure 6** shows a simplified flowchart of the wastewater treatment plant (WWTP) under study. As shown in **Figure 6**, the system comprises 6 main process steps with two main clarification units; the treatment plant combines mechanical, chemical and biological treatment [28].

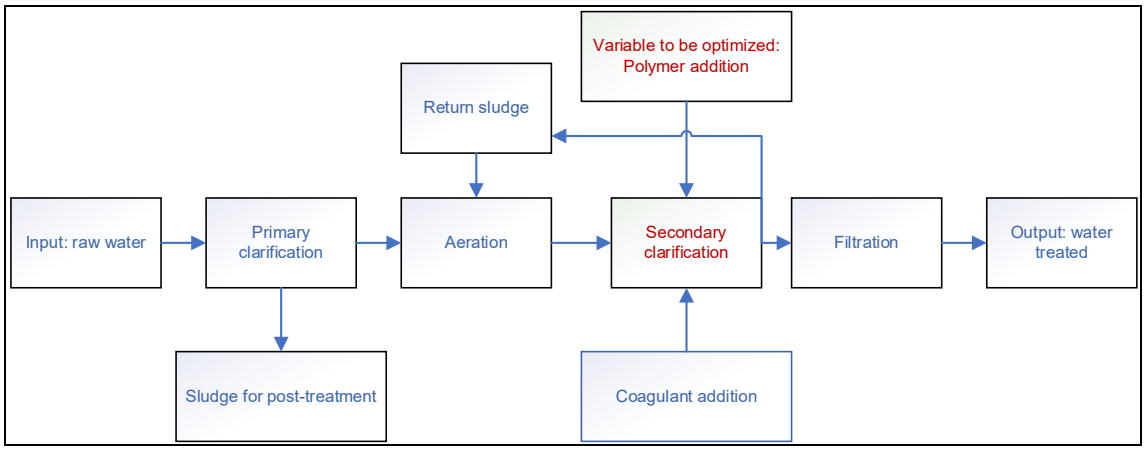

Figure 6. Simplified flowchart of the wastewater treatment plant under study (Turku Wastewater Treatment Plant, Turun Seudun Puhdistamo)

The first step involves the entry of raw water into the system. This raw water is pre-treated with a primary clarification step where large particles are removed. Additionally, during this step the surplus of sludge is dewatered by using polymer and centrifugation. The sludge is later stored in a silo to be sent for post-treatment. Once the primary clarification is completed, the partially treated water proceeds to the active sludge process, the first treatment of which consists of aeration. For this operation, 7 sub-treatment blocks are employed: 2 corresponding to the anoxic treatment, 3 for the aerobic treatment, one combined anoxic/aerobic treatment block, and finally the degasification block. Subsequently, the effluent goes to the secondary clarification unit where the coagulant (ferrous sulphate) and flocculant (cationic polymer) are added. It should be noted that the output sludge is recirculated into the aeration unit. Finally, the water goes to a final tertiary step constituted by several filtration blocks, after which the treated water is released into the Baltic Sea. The sludge is processed using anaerobic digestion, generating about 30 GWh of energy per year [28].

The calculation of the chemical process indicator was performed for the secondary clarification unit. Therefore, the optimisation of the flocculation concentration was based on the analysis of the concentration of phosphorus, total suspended particles, and sedimentation kinetics. Meanwhile, the calculation of the cost associated with the energy consumption of the plant accounts for the whole process.

RESULTS AND DISCUSIONS

Figure 7a illustrates the influence of time on the evolution of the peak thickness after addition of the polymer solution at different concentrations, obtained from the sample "20/02/2023": In contrast, Figure 7b displays the time evolution of the peak thickness for the different data set. As observed, the peak thickness of the water sample collected on 20/02/2023 differs by several orders of magnitude compared to the other two data sets. Nevertheless, the stability plateau of the analysed samples (with and without polymer addition) is typically achieved after 100 seconds of analysis.

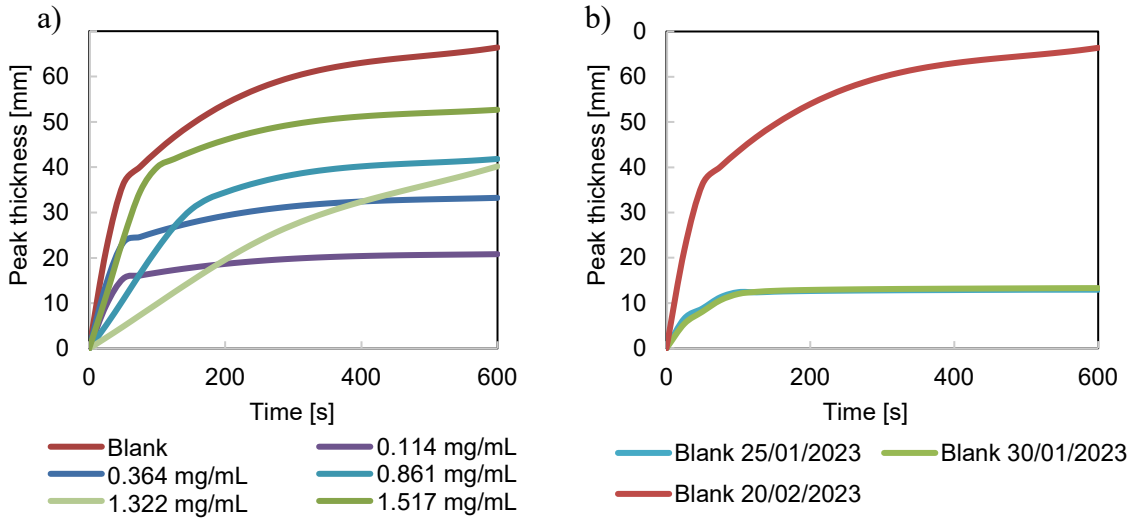

Figure 7. Time evolution of the peak thickness: a) obtained at different polymer concentration for the sample "20/02/2023" (a); of the raw water collected at different dates (b)

Therefore, to comprehend the influence of the polymer concentration on the speed of the flocculation, the variation of the peak thickness as a function of time for the initial times was calculated (**Figure 8**). Integrating the information shown in **Figure 7b** and **Figure 8**, the lowest particle migration rate of the sample set corresponds to about 10 mm of peak thickness, which can be achieved at 0.861 mg/mL of polymer. Conversely, the sample set that exhibits a peak thickness stability plateau at 64 mm required 1.322 mg/mL of polymer. Considering this last particle migration rate, less than 0.1 mm/s can be attained using only 0.114 mg/mL of polymer for the data set with initial low peak thickness. Based on the general characteristics of the water samples (**Table 1**), the only difference between those samples is the inflow volume. The inflow volume of the sample "20/02/2023" was 62% lower compared to the other two samples. Moreover, when examining the weather conditions on those days **[34]**, it can be observed that the increasing of the inflow volume was due to rain, as shown in **Figure 9** (9a represents 30/01/2023 and 9b stands for 20/02/2023). In theory, due to the rain the input water was cleaner, and this justifies why for the samples of 30/01/2023 and 25/01/2023 (gray and blue respectively in **Figure 7**b) less amount of polymer is required than for 20/02/2023, even if the initial suspended particles concentration is similar.

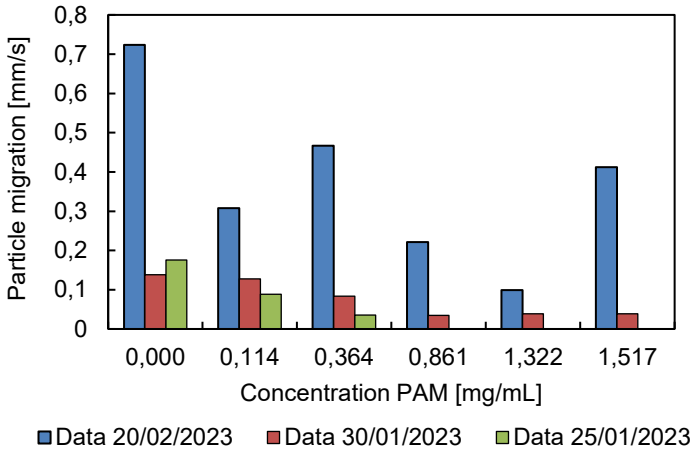

Figure 8. Evolution of the particle migration during the initial times of sedimentation as a function of the polymer concentration, obtained from different raw water samples

a)

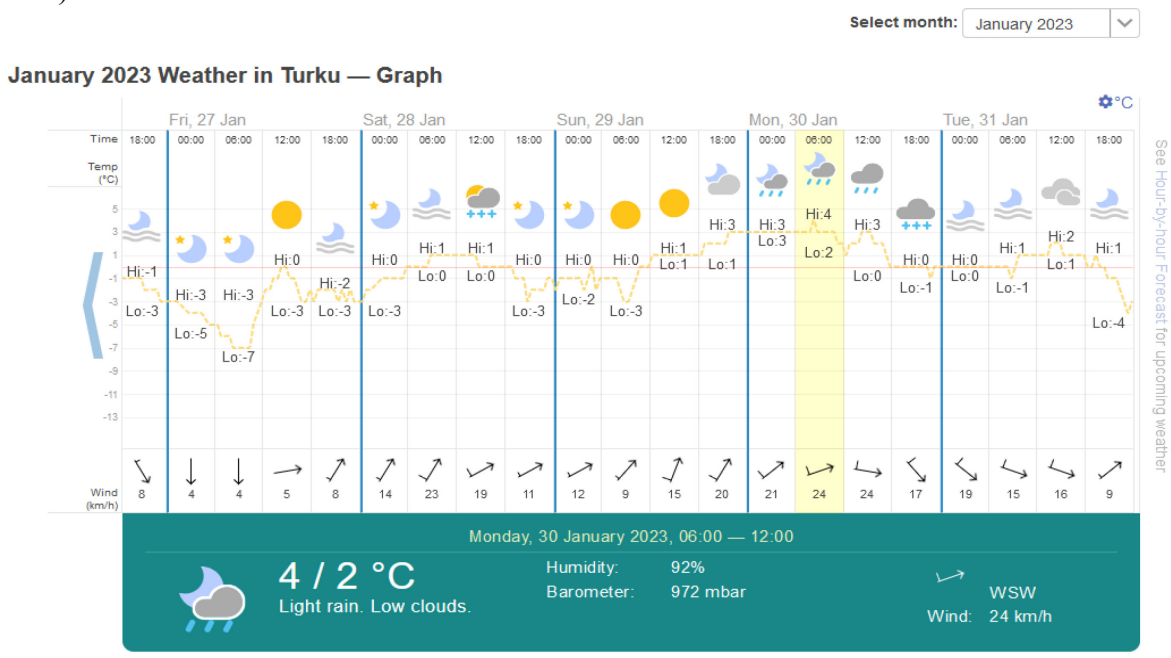

b)

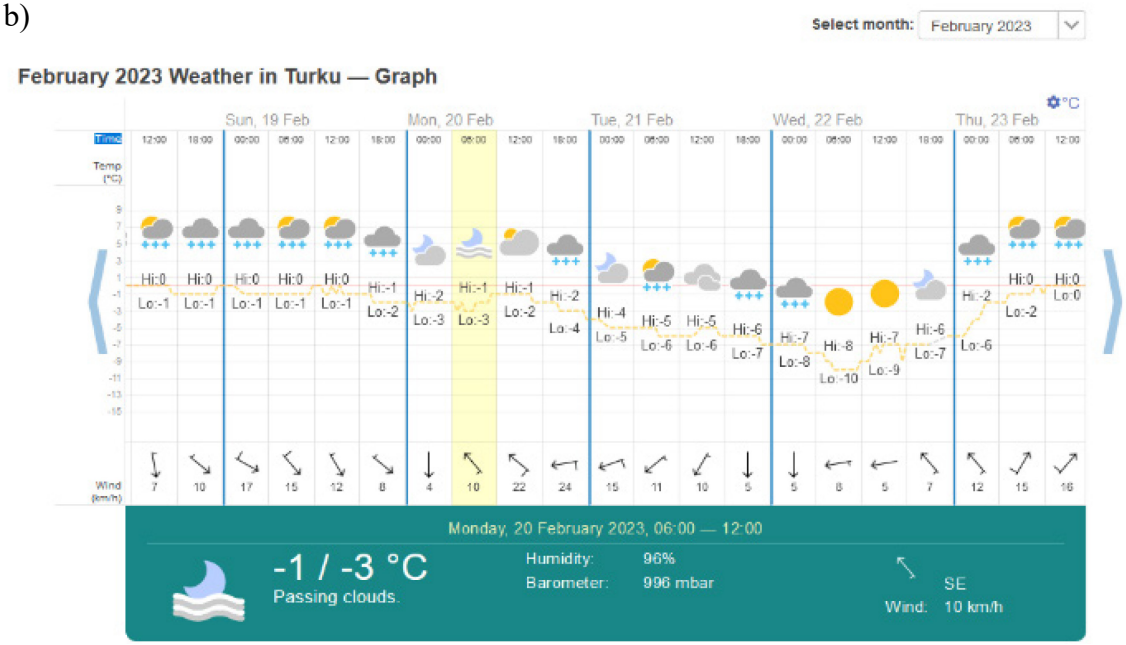

Figure 9. Past weather in Turku, Finland during two days when samples were collected: 30/01/2023 (a) and 20/02/2023 (b) [34]

Figure 10 depicts the evolution of the zeta potential as a function of the polymer concentration for the different data sets. It is noteworthy that the zeta potential reaches the isoelectric point at similar concentration of polymer, regardless of the data set studied. Flocculation between the impurities and the polymer particles can be initiated by one or simultaneous mechanisms, namely charge neutralisation, polymer bridging, and polymer-particle surface complex formation [35]. At lower concentration of polymer in the solution (up to 0.114 mg/mL), the dominant mechanism is the charge neutralisation, given the available cationic charges provided by the block structure of the polymer are high and sufficient to achieve the neutralisation of the negative charges of the wastewater. Subsequently, as the zeta potential value increases, impurities-polymer particles reach a new stabilisation stage and polymer bridging becomes the dominant mechanism.

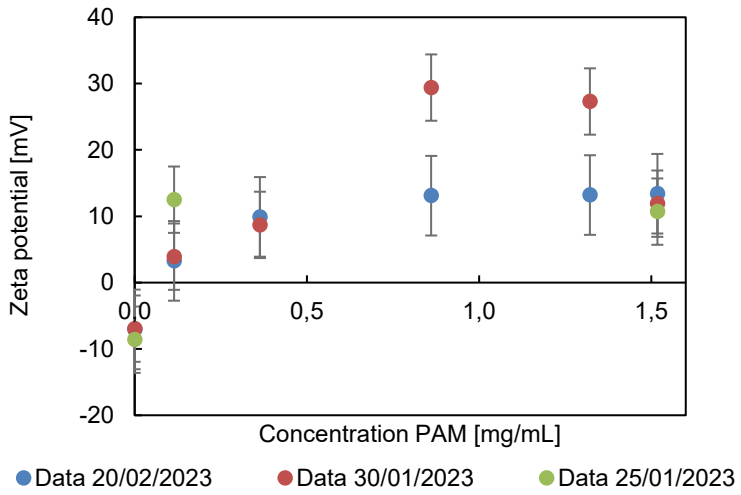

Figure 10. Evolution of the zeta potential as a function of the polymer concentration obtained from different raw water samples

Figure 11a presents the evolution of the particle size represented in terms of size class and frequency volume compatibility, while **Figure 11b** displays the measured particle sizes. As observed, the evolution of the particle size progresses in a stepwise manner. In the absence of flocculant, the mean particle size is 190 µm.

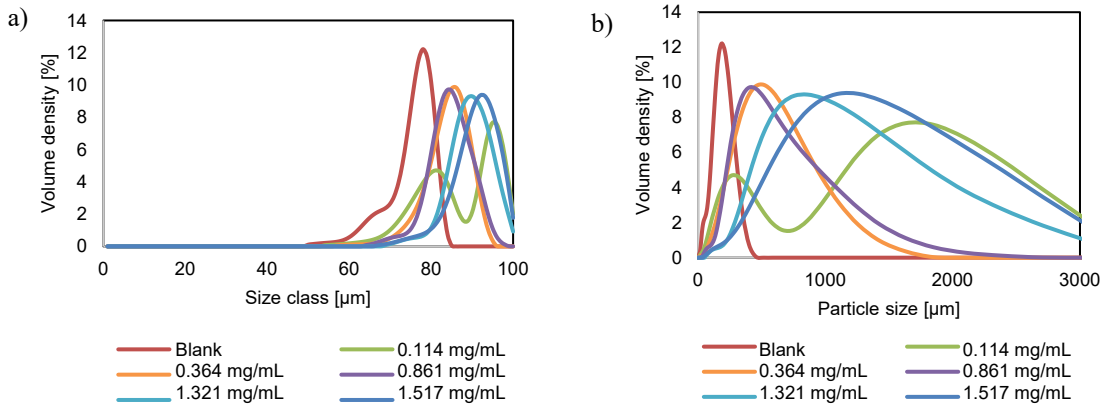

Figure 11. Evolution of the size classes (a) and particle size as a function of the polymer concentration (b)

When the concentration of polymer is around 0.114 mg/mL, two populations of mean particle size of 210 µm and 1630 µm can be identified. After 0.364 mg/mL, one population with a mean particle size of 450 µm dominates until the concentration is increased to 1.321 mg/mL, achieving particle size higher than 760 µm. Correlating this data with the zeta potential, insights about the stability of the system can be gained. It can therefore be stated that for concentration below 0.114 mg/mL, the system is in transition, evidenced by the zeta potential close to 0 mV and by the presence of two populations. Then, after increasing the concentration up to 0.364 mg/mL, the system attains another stability state by reaching zeta potential values of about 10 mV. The maximum stability occurs around 0.861 mg/mL, which appears to be the best concentration for promoting the flocculation mechanism. At this point, the flocs are large enough to promote the phase separation in the clarification unit and stable enough to be processed.

Undoubtedly, the kinetic of sedimentation needs to be understood by considering the contribution of one population at a time. In this sense, one population will record a specific sedimentation speed and its general contribution to the total sedimentation of the system will depend on the concentration of the suspended impurities particles and how they interact with the polymer particles. **Figure 12** demonstrates the impact of the storage time on the kinetics of sedimentation. In absence of agitation, the aggregates are partially sedimented and even if the impurities particles are not "strongly" attached among them, the polymer bridging mechanism is favoured under those conditions. Therefore, a lower polymer concentration is required to achieve optimal flocculation conditions. As expected, the residence time and turbulence are key parameters on the flocculation formation mechanism. Nevertheless, increasing the residence time implies not only a reduction of the production time, but also a surplus in the inflow volume, increasing the risk of overload. Adapting the system's residence time at a slower pace during low-inflow periods can therefore further reduce the need for polymer use and may slightly reduce electricity consumption in pumps by demanding lower internal flow.

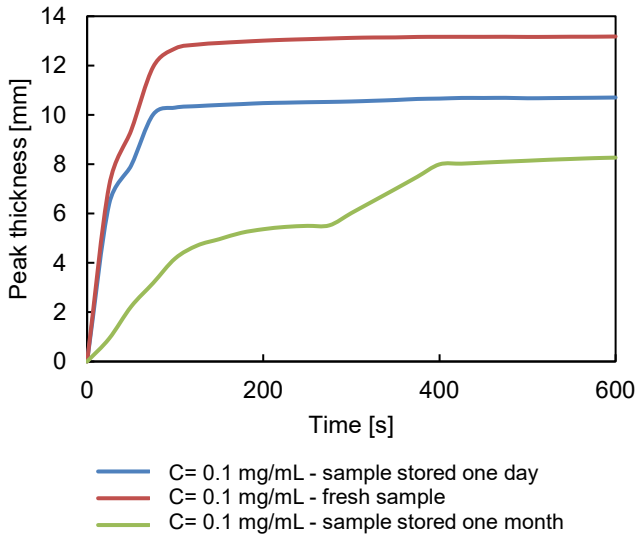

Figure 12. Influence of storage time on the evolution of the peak thickness obtained at the same initial polymer concentration

Up this point and in agreement with the literature **[36]**, the predominant mechanisms of the flocculation of the wastewater using cationic polyacrylamide are the charge neutralisation and the interaction between polymer and impurities via polymer bridging. Based on the two minimum found in the flocculation rate, charge neutralisation takes place at concentration around 0.114 mg/mL, while the polymer bridging takes place at 1.321 mg/mL. Indeed, the system is evolving, therefore re-conformation process is continuously occurring, so the competition between the mechanism can be dependent on the particle size, nature, and even related to the storage of the sample.

Figure 13 demonstrates the influence of the concentration of polymer on the ion's removal. For this study, the concentration of phosphorus, sodium and sulphur were measured. The concentration of phosphorus, nitrogen and sulphur **[36]** are of interest due to the potential eutrophication effect that the chemical modification **[37]** of those ions can have on the environment **[38]**. Here, notable differences were observed in the phosphorus concentration, and as illustrated in **Figure 13**, 0.030 mg/mL of polymer is sufficient to lower the concentration of phosphorus from 5.525 mg/mL to 0.308 mg/mL. The initial sulphur charge was already under the detection limit of the ICP-OES measurement, i.e., 3 mg/100 g; and the concentration of sodium varied between 2.0 mg/100 g and 1.2 mg/100 g. Given that a portion of this study

was conducted during wintertime and cities tend to use road salt to prevent the road icing, information about the concentration of sodium is also valuable. In fact, a higher concentration of sodium might affect not only on the permeability of the soils, but also the reduction of oxygen content in the receiving waterbody [7].

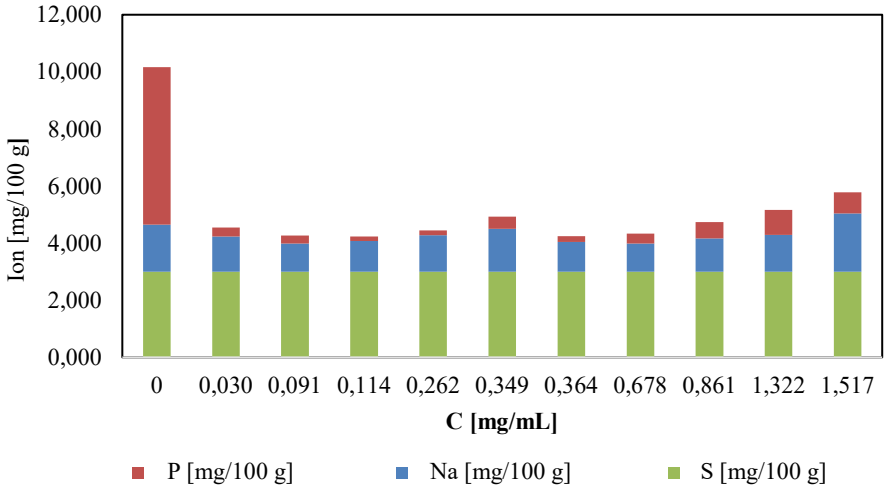

Figure 13. Evolution of the contaminant's concentration in presence of polymer.

From the battery's perspective, the total capital investment (CAPEX) required for the battery's installation is 169 million € over an expected operational lifetime of 20 years. This figure takes into account a 2% interest rate, a 1.1 USD/€ exchange rate, and battery costs as projected for 2025 from [39]. The lifetime benefit of operating the battery (considering 2022 for electricity market price variations) for Scenario 1 is estimated at 106.9 million € in energy savings, while for Scenario 2, the calculation yields 73.8 million € in revenue from electricity sales. Thus, under the current assumptions, the battery is not a profitable venture, as the benefits in both cases fall below the investment level. However, the battery offers additional benefits that are not economically measurable, such as system resiliency and back up, as well as grid stability. Moreover, several of the assumed factors used for the economic calculations are susceptible to variations that could make the battery profitable, such as different battery technology, different interest rates, an accelerated technology learning curve, and specifically for Scenario 2, a lower fixed-price agreement. The results of the financial calculations are presented in **Table 2**.

Table 2. Results of the financial analysis for battery implementation (exchange rate 1.1 USD/€)

	Scenario 1	Scenario 2
Battery power [MW]	18	
Storage capacity [MWh]	480	
Power cost [USD/kW]	1600	
Storage cost [USD/kWh]	200	
Interest rate [%]	2%	
Lifetime [years]	20	
CAPEX [M€]	169	
Lifetime benefit [M€]	106.9	73.8

As shown in **Table 2**, and under the presented assumptions, different benefits are obtained from the battery operation modes as described in Scenarios 1 and 2. Although the battery dimensions, and thus investment, are equal for Scenario 1 and 2, the benefits manifest in

different forms and at different values. For Scenario 1, there is no trade of electricity back to the grid, so the entirety of the benefit comprises electricity cost savings when comparing the electricity paid to the hourly electricity market price that would otherwise be paid. In contrast, Scenario 2 yields in the form of revenue, by selling electricity back to the grid at the times where profit could be made, as the difference between the fixed price and market electricity price. Since the capital investment of 169 M€ is higher than the benefits that could be obtained by either scenario, the installation of such a system is not economically viable but it can be justified in the current international context that Finland is facing.

CONCLUSIONS

Recognising the critical relationship between water and energy is key to achieving sustainable resource management. Wastewater treatment, being a highly energy-consuming process, offers a significant opportunity for optimisation. This study identifies a significant gap in the current practices, despite the well-established nature of typical wastewater treatment processes that have been in use for decades. Even the most state-of-the-art facilities present potential for improvement. This study introduces two innovative approaches aimed at optimising the operation of wastewater treatment plants. These approaches are applied to a real-world case study: a wastewater treatment plant in Turku, Finland.

The first strategy is centred on the optimisation of polymer usage during the secondary clarification phase. Implementation of this methodology could potentially lead to an enhancement in the efficiency of wastewater treatment processes. The second strategy proposes the incorporation of a grid-scale battery to mitigate electricity costs. This approach not only ensures uninterrupted operation of the plant but also significantly curtails energy expenditures. Collectively, these strategies contribute to the advancement of operational efficiency and cost-effectiveness in wastewater treatment plants.

Optimising the use of polymer in wastewater treatment is a multifaceted process. To comprehend the primary mechanisms influencing the flocculation of impurities using polymer, it is advantageous to combine zeta potential measurement with particle migration using turbidity measurements. The optimal amount of polymer can then be modulated based on various factors. A key finding of this study is that a polymer concentration of merely 0.030 mg/mL can significantly reduce the phosphorus concentration from 5.525 mg/mL to 0.308 mg/mL. This reduction plays a crucial role in mitigating the potential eutrophication effect on the environment.

The choice of flocculation mechanism − charge neutralisation using high cationic polymer or polymer bridging using a long chain polymer − depends on the specific objective. Charge neutralisation is preferred when the goal is to reduce polymer concentration, while polymer bridging is favoured for achieving larger and more stable flocs. Factors such as mixing, and shear can influence the competition between these mechanisms by altering particle collision. The storage time also plays a significant role in the kinetics of sedimentation and flocculation formation. By adapting the system's residence time at a slower pace during low-inflow periods, the need for polymer use can be further reduced. This adaptation may also slightly decrease electricity consumption in pumps by demanding lower internal flow.

The proposed grid-scale battery system, while not presenting an economic benefit under the current assumptions analysed, offers additional benefits beyond those of an economic nature. For instance, the presence of a grid-scale battery at the WWTP facility ensures uninterrupted operation of the plant during extended periods of power disruptions. Depending on the battery's lifetime point, the Depth of Discharge (DoD) allowed in the event of an extended power interruption, and the current state of charge, the battery could power the WWTP for over 30 hours on a full charge. If non-essential systems are further disconnected (e.g., the geothermal heat pump), the battery could power the WWTP for over 7 days, maintaining its essential operation even in cases of extended power outages.

Although power outages are extremely rare in the region where the WWTP is located, the potential need for backup power could be justified in the current international context. Up until February of 2022, Finland, along with several other EU countries, had a significant energy dependency to Russia, a dependency that was bilaterally severed shortly after the invasion of Ukraine. In the following year, preparation notices for potential power outages became common in Finland, and electricity prices soared. Therefore, the consideration of backup systems for infrastructure services has now become pertinent.

In conclusion, this study underscores the potential for significant advancements in wastewater treatment processes. By optimising the use of polymer in the secondary clarification step and proposing the use of a grid-scale battery to reduce electricity costs, it has been introduced innovative approaches that could lead to more efficient and cost-effective operations. While these strategies may not present immediate economic benefits under current assumptions, they offer additional advantages such as ensuring uninterrupted operation of the plant during power disruptions and contributing to system resiliency and grid stability. Furthermore, the study highlights the importance of considering external factors such as geopolitical context and weather conditions in operational decision-making. As the field continues to evolve, further research is warranted to explore other potential areas of optimisation and to validate these findings in other real-world contexts. Ultimately, the goal is to contribute to sustainable resource management and to the resilience of wastewater treatment infrastructure in the face of changing environmental and socio-economic conditions.

ACKNOWLEDGMENTS

We acknowledge Tuomi Jouko from Turun Seudun Puhdistamo for his insightful discussion and for providing the water samples and some data used in this study. We also extend our gratitude to Luis Bezerra from Åbo Akademi for his invaluable support with the ICP-OES analysis.

NOMENCLATURE

Symbols

B_d	End-of-life battery degradation, fixed at 0.80	[-]
BD_f	Battery degradation factor, 0.20 variable linearly over the 20 years lifetime of the battery	[-]
B_p	Power of the battery	[MW]
BS	Battery storage	[MWh]
CR_{S1}	Cost reductions of Scenario 1	€
CR_{S2}	Collected revenue in Scenario 2	€
C_δ	Full cycle efficiency	[-]
DEA_p	Daily Electricity Average Price	€c/kWh
DoD	Depth of discharge	[-]
D_u	Daily usage in hours	[h]
EB_h	Effective battery hours	[h]
E_f	Electricity fixed price	[€c/kWh]
Eh_c	Electricity hourly consumption	[MW]
$EMBh_p$	Average electricity price for the X highest price hours of the day over the fixed price, accounting for battery full cycle efficiency	[€c/kWh]
FB_h	Full battery hours	[h]
FH_H	Lower-cost full hours of the day represented when the electricity is taken from the grid	[h]

FH_L	Lower-cost full hours of the day represented when the electricity is taken from the battery	[h]
HC_h	Electricity cost of the lower-cost hours 14 to 16 hours (accounting for battery degradation)	[€c]
LC_h	Electricity cost of the lower-cost hours 10 to 8 hours (accounting for battery degradation)	[€c]
LFH_{Avg}	Average price of electricity for full load battery hours	[€c/kWh]
LGH_{Avg}	Average price of electricity directly taken from the grid for the lower-cost full hours of the day	[€c/kWh]
Nth_{hPH}	N_{th} lower-cost hour when the electricity is taken from the grid	[€c/kW]
Nth_{LPH}	N_{th} lower-cost hour when the electricity is taken from battery	[€c/kW]

Abbreviations

CAPEX	Total capital investment
DoD	Depth of Discharge
EU	European Union
ICP-OES	Inductively Coupled Plasma Optical Emission Spectroscopy
PAM	Polyacrylamides
PSD	Particle Size Distribution
WWTP	Wastewater Treatment Plant

REFERENCES

1. M. A. Yurdusev and H. Ari, 'An environmental impact assessment model for water resources screening', in Environmental Software Systems: Volume 2, R. Denzer, D. A. Swayne, and G. Schimak, Eds., in IFIP Advances in Information and Communication Technology., Boston, MA: Springer US, 1997, pp. 110–117, https://doi.org/10.1007/978-1-5041-2869-8_14.
2. A. Hospido, M. T. Moreira, M. Fernández-Couto, and G. Feijoo, 'Environmental performance of a municipal wastewater treatment plant', Int J LCA, vol. 9, no. 4, p. 261, Jul. 2004, https://doi.org/10.1007/BF02978602.
3. H. Kroiss, N. Matsché, and J. Krampe, '50 years of design and operation of large wastewater treatment plant conferences. A history of innovation and development', Water Science and Technology, vol. 84, no. 2, pp. 263–273, Jun. 2021, https://doi.org/10.2166/wst.2021.228.
4. M. Nasr, K. Mohamed, M. Attia, and M. G. Ibrahim, 'Chapter 9 - Sustainable Management of Wastewater Treatment Plants Using Artificial Intelligence Techniques', in Soft Computing Techniques in Solid Waste and Wastewater Management, R. R. Karri, G. Ravindran, and M. H. Dehghani, Eds., Elsevier, 2021, pp. 171–185, https://doi.org/10.1016/B978-0-12-824463-0.00009-4.
5. A. M. Hamiche, A. B. Stambouli, and S. Flazi, 'A review of the water-energy nexus', Renewable and Sustainable Energy Reviews, vol. 65, pp. 319–331, Nov. 2016, https://doi.org/10.1016/j.rser.2016.07.020.
6. T. Chen, M. Wang, J. Su, R. M. A. Ikram, and J. Li, 'Application of Internet of Things (IoT) Technologies in Green Stormwater Infrastructure (GSI): A Bibliometric Review', Sustainability, vol. 15, no. 18, Art. no. 18, Jan. 2023, https://doi.org/10.3390/su151813317.
7. K. Suits et al., 'Overview of the (Smart) Stormwater Management around the Baltic Sea', Water, vol. 15, no. 8, Art. no. 8, Jan. 2023, https://doi.org/10.3390/w15081623.
8. T. Deblonde, C. Cossu-Leguille, and P. Hartemann, 'Emerging pollutants in wastewater: A review of the literature', International Journal of Hygiene and Environmental Health, vol. 214, no. 6, pp. 442–448, Nov. 2011, https://doi.org/10.1016/j.ijheh.2011.08.002.

9. 'BCC Library - Report View - ENV008F'. [Accessed: Feb. 15, 2024], Available: https://academic.bccresearch.com/market-research/environment/water-and-wastewater-treatment-technologies-global-markets.html.
10. M. Samer, 'Wastewater Treatment Engineering', in Wastewater Treatment Engineering, IntechOpen, 2015, https://doi.org/10.5772/59384.
11. 'Wastewater treatment chemicals – what, why and when? | Veolia water technologies'. [Accessed: Feb. 15, 2024], Available: https://www.veoliawatertechnologies.co.uk/news/wastewater-treatment-chemicals-what-why-and-when.
12. N. H. S. Abdullah, M. N. Karsiti, and R. Ibrahim, 'A review of pH neutralization process control', in 2012 4th International Conference on Intelligent and Advanced Systems (ICIAS2012), Kuala Lumpur, Malaysia: IEEE, Jun. 2012, pp. 594–598, https://doi.org/10.1109/ICIAS.2012.6306084.
13. 'Foam Control Solutions for Wastewater Treatment | Veolia'. [Accessed: Feb. 15, 2024], Available: https://www.watertechnologies.com/products/wastewater-treatments/antifoaming-defoaming-agents.
14. N. K. Shammas, 'Coagulation and Flocculation', in Physicochemical Treatment Processes, L. K. Wang, Y.-T. Hung, and N. K. Shammas, Eds., in Handbook of Environmental Engineering., Totowa, NJ: Humana Press, 2005, pp. 103–139, https://doi.org/10.1385/1-59259-820-x:103.
15. S. Biggs, M. Habgood, G. J. Jameson, and Y. Yan, 'Aggregate structures formed via a bridging flocculation mechanism', Chemical Engineering Journal, vol. 80, no. 1, pp. 13–22, Dec. 2000, https://doi.org/10.1016/S1383-5866(00)00072-1.
16. T. Swift, L. Swanson, A. Bretherick, and S. Rimmer, 'Measuring poly(acrylamide) flocculants in fresh water using inter-polymer complex formation', Environ. Sci.: Water Res. Technol., vol. 1, no. 3, pp. 332–340, May 2015, https://doi.org/10.1039/C4EW00092G.
17. S. F. Hubbard, R. A. Potyrailo, P. Schottland, and V. Thomas, 'Tagging materials for polymers, methods, and articles made thereby', US6514617B1, Feb. 04, 2003 [Accessed: May 02, 2022], Available: https://patents.google.com/patent/US6514617B1/en.
18. W. Whipple, P. Reed, and W. Ward, 'Fluorescent water-soluble polymers', US20010018503A1, Aug. 30, 2001 [Accessed: May 02, 2022], Available: https://patents.google.com/patent/US20010018503A1/en.
19. T. Swift, C. C. Seaton, and S. Rimmer, 'Poly(acrylic acid) interpolymer complexes', Soft Matter, vol. 13, no. 46, pp. 8736–8744, 2017, https://doi.org/10.1039/C7SM01787A.
20. World Health Organization, Ed., Guidelines for drinking-water quality: Fourth edition incorporating the first and second addenda. Geneva, 2022.
21. E. Santos, A. Albuquerque, I. Lisboa, P. Murray, and H. Ermis, 'Economic Assessment of Energy Consumption in Wastewater Treatment Plants: Applicability of Alternative Nature-Based Technologies in Portugal', Water, vol. 14, no. 13, Art. no. 13, Jan. 2022, https://doi.org/10.3390/w14132042.
22. S. Revollar, P. Vega, R. Vilanova, and M. Francisco, 'Optimal Control of Wastewater Treatment Plants Using Economic-Oriented Model Predictive Dynamic Strategies', Applied Sciences, vol. 7, no. 8, Art. no. 8, Aug. 2017, https://doi.org/10.3390/app7080813.
23. A. Chadly, E. Azar, M. Maalouf, and A. Mayyas, 'Techno-economic analysis of energy storage systems using reversible fuel cells and rechargeable batteries in green buildings', Energy, vol. 247, p. 123466, May 2022, https://doi.org/10.1016/j.energy.2022.123466.
24. M. H. Mostafa, S. H. E. Abdel Aleem, S. G. Ali, Z. M. Ali, and A. Y. Abdelaziz, 'Techno-economic assessment of energy storage systems using annualized life cycle cost of storage (LCCOS) and levelized cost of energy (LCOE) metrics', Journal of Energy Storage, vol. 29, p. 101345, Jun. 2020, https://doi.org/10.1016/j.est.2020.101345.

25. H. Ibrahim, A. Ilinca, H. Ibrahim, and A. Ilinca, 'Techno-Economic Analysis of Different Energy Storage Technologies', in Energy Storage - Technologies and Applications, IntechOpen, 2013, https://doi.org/10.5772/52220.
26. O. Dolotko et al., 'Universal and efficient extraction of lithium for lithium-ion battery recycling using mechanochemistry', Commun Chem, vol. 6, no. 1, pp. 1–8, Mar. 2023, https://doi.org/10.1038/s42004-023-00844-2.
27. 'Turun seudun puhdistamo "Turku Region Wastewater Treatment Plant Ltd.)', Turun Seudun Puhdistamo. [Accessed: Mar. 23, 2023], Available: https://www.turunseudunpuhdistamo.fi/in-english.
28. 'Circular Turku - A Roadmap Toward Resource Wisdom', European Circular Economy Stakeholder Platform. [Accessed: Feb. 27, 2024], Available: https://circulareconomy.europa.eu/platform/en/strategies/circular-turku-roadmap-toward-resource-wisdom.
29. 'Exchange electricity spot price in Finland', Sahko TK. [Accessed: Mar. 23, 2023], Available: https://sahko.tk.
30. M. I. Hlal, V. K. Ramachandaramurthy, A. Sarhan, A. Pouryekta, and U. Subramaniam, 'Optimum battery depth of discharge for off-grid solar PV/battery system', Journal of Energy Storage, vol. 26, p. 100999, Dec. 2019, https://doi.org/10.1016/j.est.2019.100999.
31. D. Gräf et al., 'What drives capacity degradation in utility-scale battery energy storage systems? The impact of operating strategy and temperature in different grid applications', Journal of Energy Storage, vol. 47, p. 103533, Mar. 2022, https://doi.org/10.1016/j.est.2021.103533.
32. V. Ramasamy et al., 'U.S. Solar Photovoltaic System and Energy Storage Cost Benchmarks, With Minimum Sustainable Price Analysis: Q1 2022', NREL/TP-7A40-83586, 1891204, MainId:84359, Sep. 2022, https://doi.org/10.2172/1891204.
33. IRENA, 'Electricity storage and renewables: Costs and markets to 2030', , International Renewable Energy Agency, 2017, Abu Dhabi.
34. Timeanddate, 'Weather in January 2023 in Turku, Finland'. [Accessed: Mar. 30, 2023], Available: https://www.timeanddate.com/weather/finland/turku/historic?month=1&year=2023.
35. Q. Guan et al., 'Effect of Template on Structure and Properties of Cationic Polyacrylamide: Characterization and Mechanism', Ind. Eng. Chem. Res., vol. 53, no. 14, pp. 5624–5635, Apr. 2014, https://doi.org/10.1021/ie404116k.
36. L. Feng, M. Kobayashi, and Y. Adachi, 'Initial stage dynamics of bridging flocculation of polystyrene latex particles with low charge density polycation in a mixing flow near the isoelectric point', Colloid Polym Sci, vol. 293, no. 12, pp. 3585–3593, Dec. 2015, https://doi.org/10.1007/s00396-015-3729-y.
37. B. Raue, H.-J. Brauch, and F. H. Frimmel, 'Determination of sulphate in natural waters by ICP/OES — comparative studies with ion chromatography', Fresenius J Anal Chem, vol. 340, no. 6, pp. 395–398, Jun. 1991, https://doi.org/10.1007/BF00321590 .
38. J. Vartainen and M. Arve, 'Clean, productive and shared Baltic Sea', The Baltic Sea Challenge. [Accessed: Feb. 27, 2024], Available: https://itamerihaaste.fi/en/etusivu.
39. 'Utility-Scale Battery Storage', NREL Transfroming Energy. [Accessed: Mar. 23, 2023], Available: https://atb.nrel.gov/electricity/2022/utility-scale_battery_storage.

Paper submitted: 12.04.2024
Paper revised: 02.07.2024
Paper accepted: 03.07.2024